International Journal of Solids and Structures 45 (2008) 4375–4383

Contents lists available at ScienceDirect

International Journal of Solids and Structures

journal homepage: www.elsevier.com/locate/ijsolstr

# On computation of the compliance and stiffness contribution tensors of non ellipsoidal inhomogeneities

I. Sevostianov [a,*], M. Kachanov [b], T. Zohdi [c]

[a] Department of Mechanical and Aerospace Engineering, New Mexico State University, P.O. Box 30001, Las Cruces, NM 88003, USA
[b] Department of Mechanical Engineering, Anderson Hall, Tufts University, Medford, MA 02153, USA
[c] Department of Mechanical Engineering, 6195 Etcheverry Hall, University of California, Berkeley, CA 94720-1740, USA

ARTICLE INFO

*Article history:*
Received 27 November 2007
Received in revised form 18 March 2008
Available online 31 March 2008

*Keywords:*
Compliance contribution tensor
Elasticity
Effective properties

ABSTRACT

We discuss computation of compliance/stiffness contribution tensors of an inhomogeneity of non-ellipsoidal shape and the difficulties that may be encountered in this context. These issues are illustrated on the example of one specific shape factor: concavity–convexity of the inhomogeneity shape. It is found, in particular, that the effect of the concavity factor depends on the specific constraint imposed. If the inhomogeneity volume is kept constant, then its compliance contribution rapidly increases with increasing concavity; on the computational side it leads to difficulties related to unusually high requirements to the accuracy of the computed volume averages quantities. If, on the other hand, the characteristic dimensions (for example, the distance between the farthest points) are kept constant, then the dependence of the compliance contribution on the concavity factor is almost linear.



## 1. Introduction

In the problem of effective elastic properties of heterogeneous materials, of key importance is finding the contribution of a single inhomogeneity into the overall compliance. The available analytical results in this area are limited to the ellipsoidal shapes since they are based on Eshelby's theory (1957). In materials science applications, however, inhomogeneities may have irregular (non-ellipsoidal) shapes. It is of importance therefore to examine the effects of various shape factors – such as shape concavity–convexity – on the inhomogeneity compliance contribution.

In the case of "irregular" shapes, shape factors cannot be ignored even in the case when the compliance contribution of the inhomogeneity is isotropic: the effect of the inhomogeneity on two elastic parameters – bulk and shear moduli – cannot be characterized by adjusting one concentration parameter. Even in the cases when such a characterization can be done with some approximation, the concentration parameter has to be treated as an *adjustable* one (although this is not always acknowledged), so that link to microstructure is lost. Geophysics applications provide many examples of this kind: although cracks in rocks typically have highly irregular shapes, their density is routinely described in terms of the usual crack density parameter that is defined for the *circular* shapes ($e = (1/V)\sum a^{(k)3}$ where $a^{(k)}$ is radius of $k$th crack) and the only option left is to treat $e$ as a fitting parameter.

The problem of "irregular" (non-ellipsoidal) inhomogeneities requires computational approaches. They can be generally classified as follows:

* Corresponding author. Tel.: +1 505 6463322; fax: +1 505 6466 111.
*E-mail addresses:* igor@nmsu.edu (I. Sevostianov), mark.kachanov@tufts.edu (M. Kachanov), Zohdi@me.berkeley.edu (T. Zohdi).

0020-7683/$ - see front matter 
doi:10.1016/j.ijsolstr.2008.03.020

- Direct computation of stress and strain fields for a given (deterministic) microstructure by discretizing the domain and using the FEM, and then post-processing the averages of the stress and strain fields (see, for example, Arns et al., 2002).
- Computation of the contribution of one isolated inhomogeneity into the effective elastic properties as a function of its shape. Such results constitute basic building blocks for theoretical models that cover diverse orientation distributions and concentrations of inhomogeneities.

The present work focuses on the second approach. It may seem that the mentioned contributions can be computed in a straightforward way: an inhomogeneity of volume $V_*$ is placed in a certain volume $V$ (where $V \gg V_*$, so that perturbations of fields due to the inhomogeneity are negligible on $\partial V$). Volume $V$ is then subjected to homogeneous boundary conditions (in absence of the inhomogeneity, the fields would have been uniform within its site) and averages of fields over $V$ are computed by the finite element method. However, this approach may lead to large errors, rooted in the fact that extraction of the inhomogeneity contribution from average over $V$ quantities involves amplification of numerical errors by a very large factor $V/V_*$. These issues are discussed in the present work, with particular attention paid to the concave shapes.

We consider homogeneous matrix containing an isolated pore, and denote the compliance and stiffness tensors of the matrix by $\boldsymbol{S}^0$, $\boldsymbol{C}^0$. As discussed in Section 4, the results for the compliance contribution of a pore can be recalculated for an inhomogeneity of the same shape but with arbitrary elastic properties.

Representing the average over volume $V$ strain generated by applied stress $\boldsymbol{\sigma}^\infty$ as a sum

$$\boldsymbol{\varepsilon} = \boldsymbol{S}^0 : \boldsymbol{\sigma}^\infty + \Delta\boldsymbol{\varepsilon} \tag{1}$$

reduces the problem to expressing extra strains $\Delta\boldsymbol{\varepsilon}$, per volume $V$, due to the presence of the pore in terms of $\boldsymbol{\sigma}^\infty$.

In the framework of linear elasticity, $\Delta\boldsymbol{\varepsilon}$ is a linear function of $\boldsymbol{\sigma}^\infty$:

$$\Delta\boldsymbol{\varepsilon} = \boldsymbol{H} : \boldsymbol{\sigma}^\infty \tag{2}$$

where fourth-rank tensor $\boldsymbol{H}$ is the compliance contribution tensor of the inhomogeneity.

For an ellipsoidal inhomogeneity, $\boldsymbol{H}$ tensor is expressed in terms of Eshelby's tensor (see, for example, Sevostianov and Kachanov, 2002). In 2D case, components of $\boldsymbol{H}$-tensors were computed for a number of shapes using the complex variables technique (Zimmerman, 1986; Kachanov et al., 1994; Tsukrov and Novak, 2002, 2004; Ekneligoda and Zimmerman, 2006). Needs of materials science call for analyses of various "irregular" 3D geometries. Although some results of this kind are available for cracks (Sevostianov and Kachanov, 2002; Grechka et al., 2006; Mear et al., 2007), the case of pores and inclusions is much less explored.

## 2. On two possible ways of normalizing the compliance contribution tensor

The compliance contribution tensor of an inhomogeneity is proportional to its volume $V_*$ or, alternatively, to $L_*^3$ where $L_*$ is certain characteristic length of the inhomogeneity (for example, the maximal distance between its far points). However, the knowledge on the compliance contribution tensors of inhomogeneities should be presented in the size-independent form, *i.e.* in terms of tensors $\overline{\boldsymbol{H}}$ that reflect the shape – but not the size – of the inhomogeneity considered:

$$\boldsymbol{H} = \frac{L_*^3}{V}\overline{\boldsymbol{H}} \tag{3}$$

Alternatively, one may replace

$$L_*^3 \to V_* \tag{4}$$

i.e. to normalize $\boldsymbol{H}$ to the volume of the inhomogeneity; such a normalization may seem attractive since there is no universal procedure for identifying $L_*$ of a given shape:

$$\boldsymbol{H} = \frac{V_*}{V}\overline{\boldsymbol{H}} \tag{5}$$

We emphasize that $\overline{\boldsymbol{H}}$ tensors entering the two relations, (3) and (5), are different: they represent different normalizations of $\boldsymbol{H}$ – to $L_*^3$ and to $V_*$, respectively. In the text to follow, we discuss the choice between the two.

First, we note that for certain shapes the volume normalization (5) is inappropriate since large changes in their volume $V_*$ have only minor effect on their compliance contribution. An example is given by a pore of strongly oblate spheroidal shape (semiaxes $a_1 = a_2 \gg a_3$), with aspect ratio $\gamma = a_3/a_1 \ll 1$. The dependence of components of $\boldsymbol{H}$ on $\gamma$ is shown in Fig. 1. Changes in $\gamma$ of the order of 0.05 produce smaller than 10% changes in all $H_{ijkl}$. Moreover, in the vicinity of $\gamma = 0$ (slightly "inflated" crack), 12 out of 21 components are very small; therefore, being measured in the Euclidean norm, the deviation of $\boldsymbol{H}$ from its value for a *crack* is below 10% up to $\gamma = 0.10$. From the computational viewpoint, normalization to inhomogeneity volume $V_*$ may lead to serious computational difficulties in such cases.

**Remark 1.** The discussion above assumes the linear elastic formulation, without crack closure effects; in the case of compressive loads, this translates into the requirement that they should be sufficiently small as not to cause closure.

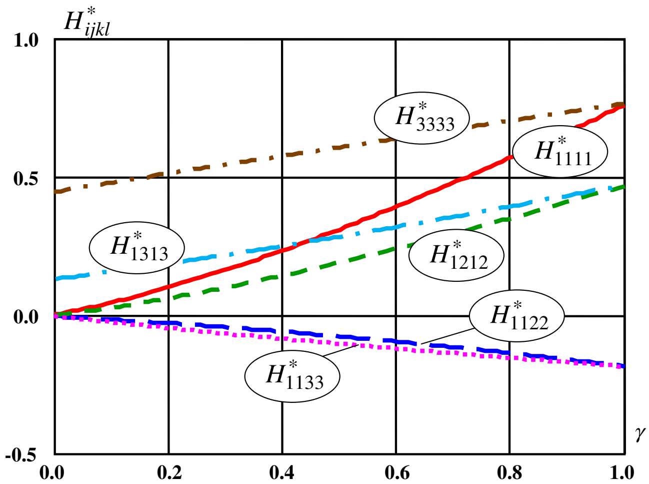


**Fig. 1.** Components of the normalized compliance contribution tensor $(E_0 a^3 H_{ijkl}/V)$ of an oblate pore as functions of its aspect ratio.

The above described limitations indicate that the normalization to $L_*^3$ may be generally preferable, in the sense that it is always applicable. In those cases when both normalizations can be used, the choice should depend on the question one wishes to answer:

*A*. One may be interested in examining the change of $\boldsymbol{H}$ as the inhomogeneity shape is changed in certain specific way. Then $\boldsymbol{H}$ should be normalized to $L_*^3$ where $L_*$ is chosen in such a way that it remains constant in the process of change. We illustrate this statement by two examples:

(a) In examining tensor $\boldsymbol{H}$ of the spheroidal pore, as a function of its aspect ratio, $L_*$ can be selected as pore radius.
(b) The shape is changed from a convex one to a concave one, while keeping the distance between far points ("vertices") fixed; see example considered in Section 4. In examining $\boldsymbol{H}$ as a function of the convexity–concavity factor, $L_*$ can be selected as the mentioned fixed distance.

In such cases, the microstructural parameter for a material with multiple inhomogeneities may not reduce to the volume fraction.

*B*. If one examines, instead, how the effect *of given volume* $V_*$ changes as its shape is changed, then $\boldsymbol{H}$ should be normalized to $V_*$. In this case, the parameter of concentration of inhomogeneities reduces to volume fraction, or its generalized form (17) that contains shape factors as parameters.

The absence of clarity in distinguishing, which question one wishes to answer – *A* or *B* – may lead to physically incorrect conclusions. An example, discussed in Section 4, is given by the convexity–concavity factor of a pore: the convexity–concavity transition is characterized by relatively slow change of $\boldsymbol{H}$; from this point of view, this shape factor is not important. However, the effect of *given pore volume* $V_*$ increases rapidly as the shape becomes concave and the distance between its far points increases correspondingly; from this point of view, the convexity–concavity factor is important.

The choice between **A** and **B**, i.e. between normalization of $\boldsymbol{H}$ to $V_*$ or to $L_*^3$, is relevant for selecting the computational methodologies. In certain cases when $V_*$ shrinks to small values, using the most frequently used computational tool – the FEM – may lead to substantial difficulties if normalization to $V_*$ is used, as discussed in Section 4.

Indeed, in the framework of the FEM, one usually computes averages over certain volume $V$ containing an inhomogeneity of volume $V_*$, so that the following quantity can be extracted:

$$\langle \varepsilon \rangle - \boldsymbol{S}^0 : \boldsymbol{\sigma}^\infty \tag{6}$$

It represents the computed value of $\boldsymbol{H} : \boldsymbol{\sigma}^\infty$ and performing calculations for several "trial" stress states $\boldsymbol{\sigma}^\infty$ would yield all the components of $\boldsymbol{H}$. The latter involves inevitable computation errors and can be represented as

$$\boldsymbol{H}_{\text{computed}} = \boldsymbol{H}_{\text{exact}} + \Delta\boldsymbol{H} \tag{7}$$

where $\Delta\boldsymbol{H}$ is the error of the computation.

In order to extract the size-independent $\overline{\boldsymbol{H}}$, the computed value (7) has to be multiplied by the ratio $V/V_*$. This ratio should be sufficiently large: for the computed tensor $\boldsymbol{H}$ to represent an isolated inhomogeneity, the fields associated with the latter must be sufficiently small on boundary $\partial V$. Practically speaking, the ratio $V/V_*$ should be at least of the order of $10^2 - 10^3$. Therefore, in extracting $\overline{\boldsymbol{H}}$ from computations

$$\overline{\boldsymbol{H}} = \frac{\boldsymbol{V}}{\boldsymbol{V}_*}\boldsymbol{H}_{computed} = \underbrace{\frac{\boldsymbol{V}}{\boldsymbol{V}_*}\boldsymbol{H}_{exact}}_{\overline{\boldsymbol{H}}_{exact}} + \frac{\boldsymbol{V}}{\boldsymbol{V}_*}\Delta\boldsymbol{H} \tag{8}$$

the error $\Delta \boldsymbol{H}$ is amplified by the large factor $V/V_*$. If, for example, the accuracy of 1% in $\overline{\boldsymbol{H}}$ is required, the accuracy of computing $\boldsymbol{H}$ should be of the order of $10^{-4} - 10^{-5}$. Similar problem arises in computation of the stiffness contribution tensor $\overline{\boldsymbol{N}} = (\boldsymbol{V}/\boldsymbol{V}_*)\boldsymbol{N}$. Such accuracy can usually be achieved for smooth convex or moderately concave shapes using standard commercial FEM codes.

However, if the shape is strongly concave, the error-amplifying factor $V/V_*$ increases markedly, resulting in much more stringent requirements to the accuracy of computing $\boldsymbol{H}$. This suggests that $\overline{\boldsymbol{H}}$ – and $\overline{\boldsymbol{N}}$ – tensors should be computed by different means. One alternative is to use the boundary element method that does not utilize volume discretization (as is done in works of Ekneligoda and Zimmerman, 2006 and Mear et al., 2007). If one chooses to use the FEM, then advanced versions of the FEM should be used, that utilize adaptively refined meshes whereby the error is reduced to a priori specified level by locally refining the mesh in the zones where the error exceeds the specified value. Such techniques have been an area of intense research activity (see works of Demkowicz et al. (1989), Oden et al. (1989), Rachowicz et al. (1989), Babuska and Suri (1990) and Babuska and Oden (2005)); however, automatic and reliable error estimators and corresponding adaptive mesh refinement of this kind are not widely available in commercial packages for 3D problems.

In the text to follow, we discuss these issues in the context of the concavity–convexity shape factor. Aside from the computational issues, this shape factor is relevant to materials science applications where inhomogeneities have strongly concave shapes (such as intergranular pores). This issue is examined on the example "generalized ellipsoid".

## 3. Results for the generalized ellipsoid and their implications

We consider a pore having the shape of "generalized ellipsoid":

$$\left(\frac{x}{a}\right)^p + \left(\frac{y}{a}\right)^p + \left(\frac{z}{a}\right)^p = 1 \tag{9}$$

Its cross-section is shown in Fig. 2a for several values of $p$. For $p > 1$, the shape is convex, for $p < 1$ it is concave. As $p$ is changed, the distance between diagonally located vertices – that can be identified with $L_*$ – remains fixed, equal to $\sqrt{3}a$. We examined the range of $p$ from 0.7 to 1.3. Although this range may seem narrow, it actually corresponds to six fold variation of the inclusion volume $V_*$ (Fig. 2b).

Figs. 3 and 4 show results of FEM calculation of the overall stiffnesses and corresponding compliances (obtained by inversion) of volume $V$ containing the pore, for two different meshes. The meshes were deliberately chosen to be insufficiently fine, so that the computational error remained distinguishable (up to 7%), in order to clearly see its amplification when the value of $\overline{\boldsymbol{H}}$ is extracted.

We examine two issues: (I) computational problems related to the mentioned error amplification, and (II) physical importance of the concavity factor.

I. Normalization of $\overline{\boldsymbol{H}}$ to $L_*^3$ produces large error amplification, up to 100 times, as seen from Fig. 5 that compares $\overline{\boldsymbol{H}}$ corresponding to the two different meshes. However, the difference between the two calculated values of $\overline{\boldsymbol{H}}$ follows the same pattern as the difference between the two calculated overall compliances of volume $V$, and it is clear that reducing the error of the original calculation from 7% to, say, 0.01% – the accuracy readily achieved by commercial FEM

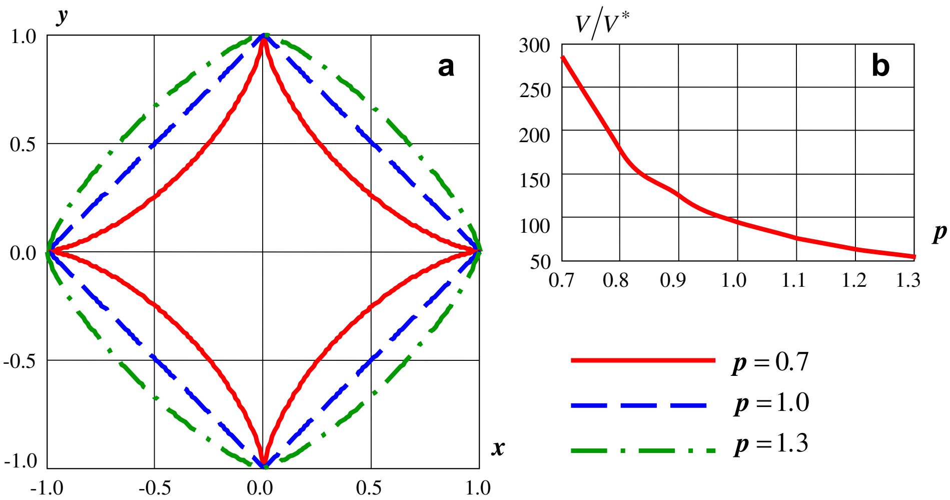


**Fig. 2.** (a) Generalized ellipsoid (formula (13)) corresponding to various values of $p$: (a) the shape of $xy$-cross-section; (b) the error amplification factor, $V/V_*$. Moderate change in $p$, from 1.3 to 0.7 results in six fold increase of $V/V_*$.

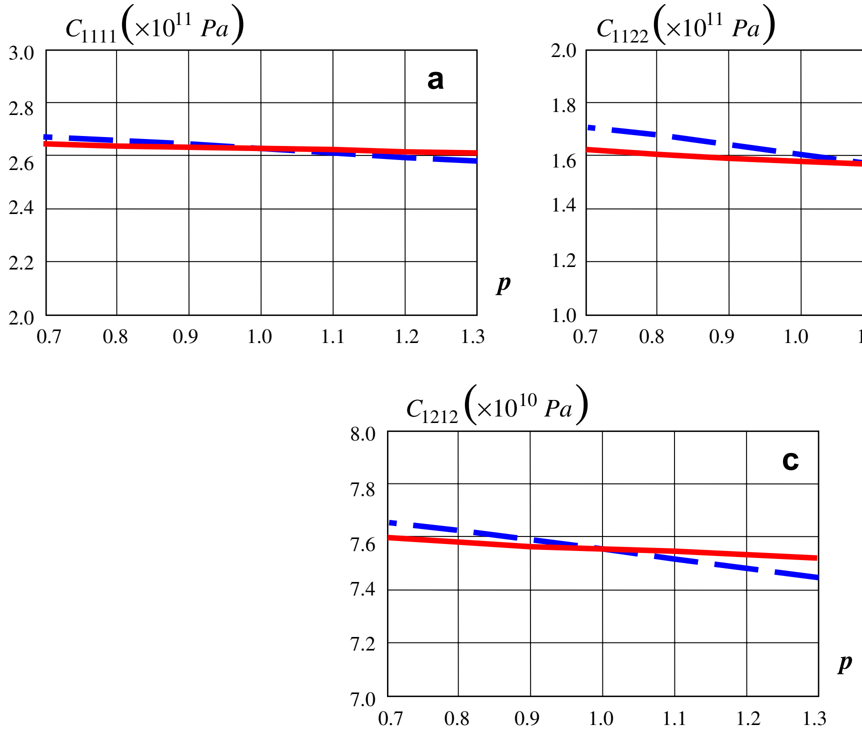


**Fig. 3.** Overall stiffnesses of volume $V$ containing single inhomogeneity having shape of generalized ellipsoid (formula (13)), as functions of parameter $p$. Solid and dashed lines correspond to two different meshes. Results of the two calculations are quite close to one another.

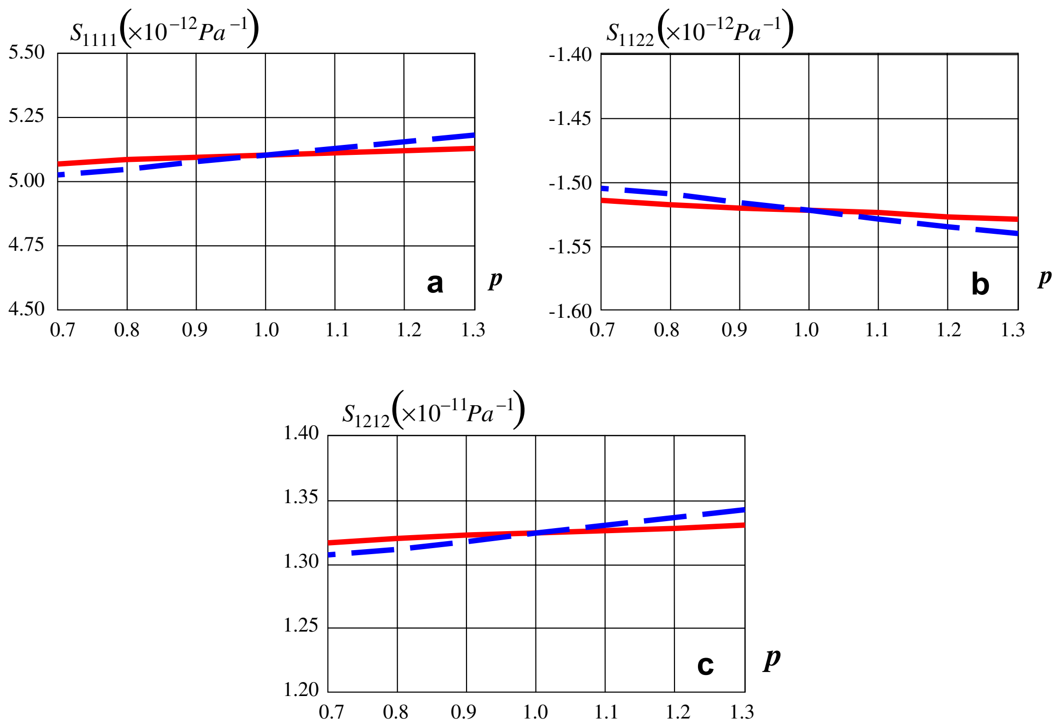


**Fig. 4.** Overall compliances of volume $V$ containing single inhomogeneity having shape of generalized ellipsoid (formula (13)), as functions of parameter $p$. Solid and dashed lines correspond to two different meshes.

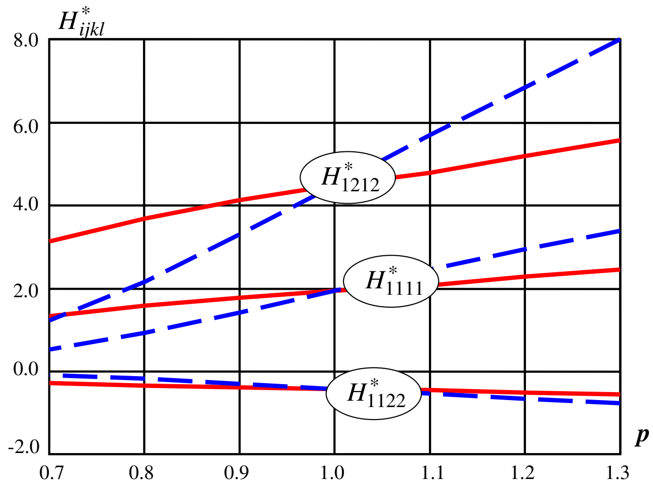


**Fig. 5.** Components of the normalized compliance contribution tensor $(E_0L_*^3H_{ijkl}/V)$. Solid and dashed lines correspond to extraction of $E_0\overline{H}_{ijkl}$ from results of the two FEM calculations (different meshes).

packages – would result in accuracy of 1% for $\overline{\boldsymbol{H}}$ that is sufficient for typical applications involving effective elastic properties. In contrast, normalization to $V_*$, besides leading to much larger errors, produces results that diverge even qualitatively for the two meshes (Fig. 6) and thus become entirely unreliable; extracting $\overline{\boldsymbol{H}}$ becomes difficult. As discussed in Section 2, this necessitates either using advanced versions of the FEM utilizing adaptively refined meshes with a priori specified error level, or alternative methodologies such as the boundary element method that do not use volume discretization.

II. As discussed in Section 2, choosing between the two normalizations – to $L_*^3$ and to $V_*$ – corresponds to answering two different questions:

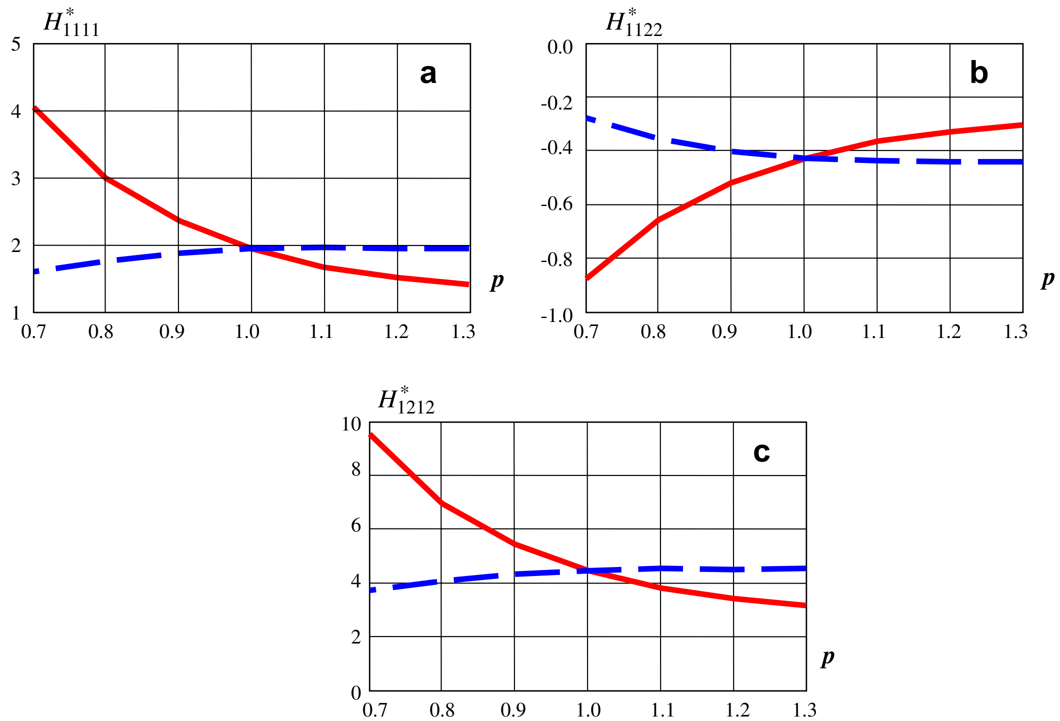


**Fig. 6.** Components of the normalized compliance contribution tensor $(E_0V_*H_{ijkl}/V)$. Solid and dashed lines correspond to extraction of $E_0\overline{H}_{ijkl}$ from results of the two FEM calculations (different meshes). It is seen that the extraction of $E_0\overline{H}_{ijkl}$ is highly unstable: the results corresponding to the two meshes are drastically different (the error of FEM calculations is amplified by the larger factor $V/V_*$).

a Normalizations to $L_*^3$ corresponds to examining the effect of concavity provided the distance between the vertices is kept constant. As seen from Figs. 3 and 4, the overall elastic properties of volume $V$ do not experience any particularly rapid changes, and, even when the error is amplified by the factor of $V/V_*$, the rate of change of components $\overline{H}_{ijkl}$ (as $p$ changes) remains approximately constant. From this point of view, the convexity–concavity transition point is of no particular importance.

b Normalization to $V_*$ corresponds to examining the effect of concavity provided the volume of the pore is fixed as $p$ changes, so that the distance between the vertices is adjusted accordingly. The mentioned distance rapidly increases as $p$ decreases (increasing concavity). Fig. 2b shows that the rate at which the volume is lost increases markedly: changing $p$ from 1.3 to 1.0 produces much smaller change in pore volume, than changing $p$ from 1.0 to 0.7. Thus, concave shapes are expected to produce much stronger effect on the overall elastic properties than convex shapes *of the same volume* as shown on the example of generalized ellipsoid (for 2D holes, this has been demonstrated, on several hole shapes, in calculations of Kachanov et al., 1994).

## 4. Discussion

We discuss the extension of our results to inhomogeneities other than pores, and their implications for the effective elastic properties of heterogeneous materials.

### 4.1. Inhomogeneities other than pores

If the material of the inhomogeneity has finite stiffness, then it may be more appropriate to express its effect on the overall elastic properties in terms of its stiffness contribution tensor: $\Delta\boldsymbol{\sigma} = \boldsymbol{N} : \boldsymbol{\varepsilon}^\infty$. Referring to Sevostianov and Kachanov (2007) for a discussion of the related issues, we note here that the formulation in terms of $\boldsymbol{H}$ tensors is generally more appropriate for cracks and pores whereas the one in $\boldsymbol{N}$ tensors is more appropriate for rigid inclusions. The issues discussed in the present work apply to $\boldsymbol{N}$-tensors as well.

In this connection, we mention the following two results:

- $\boldsymbol{H}$- and $\boldsymbol{N}$-tensors of a given inhomogeneity of any shape are interrelated as follows:

$$\boldsymbol{N} = -\boldsymbol{C}^0 : \boldsymbol{H} : \boldsymbol{C}^0, \text{ or, equivalently, } \quad \boldsymbol{H} = -\boldsymbol{S}^0 : \boldsymbol{N} : \boldsymbol{S}^0 \tag{10}$$

  or, in the case of the isotropic matrix

$$-N_{ijkl} = \lambda_0^2 H_{mmnn}\delta_{ij}\delta_{kl} + \mu_0^2 H_{ijkl} + \lambda_0\mu_0(\delta_{ij}H_{mmkl} + \delta_{kl}H_{mmij}) \tag{11}$$

  where $\lambda_0$ and $\mu_0$ are Lame constants of the matrix.

- If the material of the inhomogeneity is replaced by another one, with different elastic constants, the $\boldsymbol{H}$- and $\boldsymbol{N}$-tensors of the two inhomogeneities can be interrelated by the following "comparison" relations:

$$\left.\begin{array}{l} \frac{V_*}{V}(\boldsymbol{H}_A^{-1} - \boldsymbol{H}_B^{-1}) = (\boldsymbol{S}_A - \boldsymbol{S}^0)^{-1} - (\boldsymbol{S}_B - \boldsymbol{S}^0)^{-1} \\ \frac{V_*}{V}(\boldsymbol{N}_A^{-1} - \boldsymbol{N}_B^{-1}) = (\boldsymbol{C}_A - \boldsymbol{C}^0)^{-1} - (\boldsymbol{C}_B - \boldsymbol{C}^0)^{-1} \end{array}\right\} \tag{12}$$

  where subscripts "A" and "B" refer to two materials constituting the inhomogeneity, and $\boldsymbol{S}$ and $\boldsymbol{C}$ are the compliance and the stiffness tensors. These relations are exact for the ellipsoidal inhomogeneities or approximate, for non-ellipsoidal shapes. In particular, if material B is a *pore*, we have

$$\frac{V_*}{V}(\boldsymbol{H}_A^{-1} - \boldsymbol{H}_{\text{pore}}^{-1}) = (\boldsymbol{S}_A - \boldsymbol{S}^0)^{-1} \tag{13}$$

  This relation allows one to focus on the case of pores – as is done in the present work.

### 4.2. Implications for multiple inhomogeneities and the effective elastic properties

The issues examined in the present work have implications for the effective elastic properties of a material with multiple inhomogeneities. We represent the volume average strain generated by applied stress $\boldsymbol{\sigma}^\infty$ as a sum

$$\boldsymbol{\varepsilon} = \boldsymbol{S}^0 : \boldsymbol{\sigma}^\infty + \sum \Delta\boldsymbol{\varepsilon}^{(k)} = \boldsymbol{S}^0 : \boldsymbol{\sigma}^\infty + \sum \boldsymbol{H}^{(k)} : \boldsymbol{\sigma}^\infty \tag{14}$$

where, in the non-interaction approximation (NIA), $\boldsymbol{H}^{(k)}$ is the compliance contribution tensor of $k$th inhomogeneity considered as an *isolated* one. This identifies

$$\sum \boldsymbol{H}^{(k)} \tag{15}$$

(or, in the dual formulation, $\sum \boldsymbol{N}^{(k)}$) as the proper microstructural parameter in whose terms the effective compliances are to be expressed. The two different normalizations, to $L_*^3$ and to $V_*$ discussed above, result in two different transcriptions of this microstructural parameter:

$$\frac{1}{V}\sum L_*^{(k)3}\overline{\boldsymbol{H}}^{(\boldsymbol{k})}\ (\textit{normalization to } \boldsymbol{L}_*^{\boldsymbol{3}}) \tag{16}$$

or

$$\frac{1}{V}\sum V_*^{(k)}\overline{\boldsymbol{H}}^{(\boldsymbol{k})}\ (\textit{normalization to } \boldsymbol{V}_*) \tag{17}$$

**Remark 2.** We note that, although the discussed microstructural parameters are defined in the framework of the NIA, they are used beyond this approximation – in various effective media schemes that place non-interacting inhomogeneities into some sort of "effective environment" (effective matrix or effective stress; see, for example, review of Markov, 2000).

The first parameter, (16), can be applied to any shapes provided $L_*^{(k)}$ are chosen appropriately. For example, in the case of circular cracks, selecting $L_*^{(k)}$ as crack radii leads to the usual crack density.

The second one, (17), may be viewed as a generalized volume fraction parameter (accounting for shape factors and orientation distributions). Referring to Kachanov and Sevostianov (2005) for a discussion of microstructural parameters in detail, we mention that such parameters – tensors or scalars, in the isotropic case – have limitations. For strongly oblate or strongly concave shapes, they may be inappropriate, since volume fractions are irrelevant for them. An attempt to characterize the distribution of such pores by volume fraction type parameters would give rise to very large shape factors that tend to infinity at $\gamma \to 0$. Similar problems are encountered for strongly concave shapes. We emphasize that the computational difficulties discussed above arise in cases when the volume fraction parameters become inadequate from the physical point of view.

In spite of these limitations, the generalized volume fraction parameter (17) may be preferable in certain situations. For example, if the effective elastic properties are known, and, in addition, the volume fraction of inhomogeneities is known as well, this additional knowledge can be utilized to extract certain information on the microstructure: if volumes of individual inhomogeneities are uncorrelated with their shapes, then the average shape factor can be extracted from this information, namely $\langle\overline{\boldsymbol{H}}^{(\boldsymbol{k})}\rangle$ where the normalized compliance contribution tensors $\overline{\boldsymbol{H}}^{(\boldsymbol{k})}$ are the ones entering (17), i.e. normalized to $V_*^{(k)}$.

## 5. Conclusions

The main findings of the present work can be summarized as follows:

- In extraction of the inhomogeneity size – independent compliance contribution tensor $\overline{\boldsymbol{H}}$ from the computed overall elastic response of certain volume $V$ containing the inhomogeneity, numerical errors due to volume discretization are amplified by a very large factor for concave shapes. This factor is either $V/V_*$ or $V/L_*^3$, where $V_*$ is the inhomogeneity volume and $L_*$ is a certain characteristic length of the inhomogeneity. For the shapes that have small volume and large "profile area", such as substantially concave shapes, normalization to $V_*$ results in rapidly increasing error amplification factor as the extent of concavity increases, making the extraction of $\overline{\boldsymbol{H}}$ difficult. In these cases, normalization to $L_*^3$ is preferable. Problems of this kind do not arise, of course, if the boundary element methodologies are used.
- The effect of the concavity factor on the compliance contribution of a pore depends on the constraint imposed: is it *the distance between the far points*, or, alternatively, is it *the inhomogeneity volume* that is kept constant as the extent of concavity increases. This choice corresponds to the two different normalizations, to $L_*^3$ and to $V_*$ discussed above. As illustrated by the example of generalized ellipsoid, the convexity–concavity factor is of no particular importance in the first case. In the second case, this factor is quite important: concave shapes produce substantially larger compliance contributions than the convex shapes *of the same volume*.

## Acknowledgements

The first author (IS) acknowledges support of NASA (Contract # NNX07AD44A and Grant # GR0002488). The second author (MK) acknowledges partial support of the National Science Foundation (Grant #CMS-0509936).

## References

Arns, Ch.H., Knackstedt, M., Pinczewski, W., Garboczi, E., 2002. Computation of linear elastic properties from micrographic images: methodology and agreement between theory and experiment. Geophysics 67, 1396–1405.
Babuska, I., Oden, J.T., 2005. The reliability of computer predictions: can they be trusted? Int. J. Numer. Anal. Model. 1, 1–18.
Babuska, I., Suri, M., 1990. The p- and h-p versions of the finite element method, an overview. Comput. Meth. Appl. Mech. Eng. 80, 5–26.
Demkowicz, L., Oden, J.T., Rachowicz, W., Hardy, O., 1989. Toward a universal h-p adaptive finite element strategy. Part 1. Constrained approximation and data structure. Comput. Meth. Appl. Mech. Eng. 77, 79–112.
Grechka, V., Vasconselos, I., Kachanov, M., 2006. The influence of crack shapes on the effective elasticity of fractured rocks. Geophysics 71, D153–D160.
Ekneligoda, T.C., Zimmerman, R.W., 2006. Compressibility of two-dimensional pores having *n*-fold axes of symmetry. Proc. Roy. Soc. L A 462, 1933–1947.
Eshelby, J.D., 1957. The determination of the elastic field on an ellipsoidal inclusion and related problems. Proc. Roy. Soc. L A 241, 376–392.

Kachanov, M., Sevostianov, I., 2005. On quantitative characterization of microstructures and effective properties. Int. J. Solids Struct. 42, 309–336.
Kachanov, M., Tsukrov, I., Shafiro, B., 1994. Effective moduli of solids with cavities of various shapes. Appl. Mech. Rev. 47 (1), S151–S174.
Markov, K.Z., 2000. Elementary micromechanics of heterogeneous media. In: Markov, K.Z., Preziosi, L. (Eds.), Heterogeneous Media: Micromechanics Modeling Methods and Simulations. Birkhauser, Boston, pp. 1–162.
Mear, M., Sevostianov, I., Kachanov, M., 2007. Elastic compliances of non-flat cracks. Int. J. Solids Struct. 44, 6412–6427.
Oden, J.T., Demkowicz, L., Rachowicz, W., Westermann, T.A., 1989. Toward a universal h-p adaptive finite element strategy. Part 2. A posteriori error estimation. Comput. Meth. Appl. Mech. Eng. 77, 113–180.
Rachowicz, W., Oden, J.T., Demkowicz, L., 1989. Toward a universal h-p adaptive finite element strategy. Part 3. Design of h-p meshes. Comput. Meth. Appl. Mech. Eng. 77, 181–212.
Sevostianov, I., Kachanov, M., 2002. On the elastic compliances of irregularly shaped cracks. Int. J. Fract. 114, 245–257.
Sevostianov, I., Kachanov, M., 2007. Relations between compliances of inhomogeneities having the same shape but different elastic constants. Int. J. Eng. Sci. 45, 797–806.
Tsukrov, I., Novak, J., 2002. Effective elastic properties of solids with defects of irregular shape. Int. J. Solids Struct. 39, 1539–1555.
Tsukrov, I., Novak, J., 2004. Effective elastic properties of solids with two-dimensional inclusions of irregular shape. Int. J. Solids Struct. 41, 6905–6924.
Zimmerman, R.W., 1986. Compressibility of two-dimensional cavities of various shapes. J. Appl. Mech. 53, 500–504.